Supporting Information

Akiyama et al. 10.1073/pnas.1421949112

SI Materials and Methods

Simultaneous Cell Proliferation and Cell Death Analyses. Serial transverse sections of E9.75 embryos were stained for pHis3 and TUNEL Two sections from each of anterior, middle and posterior region per embryo were used for counting DAPI-positive nuclei, pHis3-positive and TUNEL-positive cells in the mesenchyme of nascent limb buds. Average of proliferation index (pHis3/DAPI) and cell death index (TUNEL/DAPI) of each region of three *Sall4* CKO embryos and three wild-type control embryos were used for statistical analysis by the Student's *t* test, and shown as average ± SD. *P* values are indicated within each panel.

Quantitative RT-PCR. Embryos at E9.5–E9.75 were collected and the posterior part of the body, including the hindlimb forming region/hindlimb buds, was collected. The posterior body was pushed to a plastic dish from the dorsal side by fine forceps in PBS, and tissue lateral to the somites were dissected using a fine tungsten needle. The collected tissue, termed as the lateral tissue, contains the lateral plate mesoderm/nascent hindlimb mesenchyme, surface ectoderm and some other surrounding tissue, but excluded the neural tissue, where *Irx3* and *Irx5* are expressed and *Tcre*-mediated recombination does not occur.

The lateral tissue from ~12–15 embryos with the same genotype were pooled as one group, and RNA was extracted by using RNeasy micro (QIAGEN) according to the manufacture's instruction. The reverse transcription reaction was done using SuperScript III (Invitrogen) and oligo dT primer, and quantitative PCR was done using GoTaq qPCR master mix (Promega) and a Mastercycler qPCR machine (Eppendorf). For both wild type and *Sall4* CKO genotypes, three groups were examined. Primer sequences for *Sall4*, *Irx3*, and *Irx5* were obtained from the PrimerBank (pga.mgh.harvard.edu/primerbank/index.html) (1). Relative expression levels were determined by the delta-delta Ct method with the Ct value for *Gapdh*. Statistical analysis was done by the Student's *t* test, and shown as average ± SD. *P* values are indicated within each panel.

Primer Sequences for qRT-PCR.

Sall4 FW: GAAGTGTCAAGTCCCGGTCTC

Sall4 RV: GGCTGTGCTCGGATAAATGT

Irx3 FW: GGCAATGCTTATGGGAGCGA

Irx3 RV: CGCTGTCTAAGTTTTCCAAATCG

Irx5 FW: CGCCACATCCTCGGACAAG

Irx5 RV: GCGCCGTGTAATAAAGAGGC

Gapdh FW: CAATGACCCCTTCATTGACC

Gapdh RV: GATCTCGCTCCTGGAAGATG

1. Wang X, Spandidos A, Wang H, Seed B (2012) PrimerBank: A PCR primer database for quantitative gene expression analysis, 2012 update. *Nucleic Acids Res* 40(Database issue): D1144–D1149.

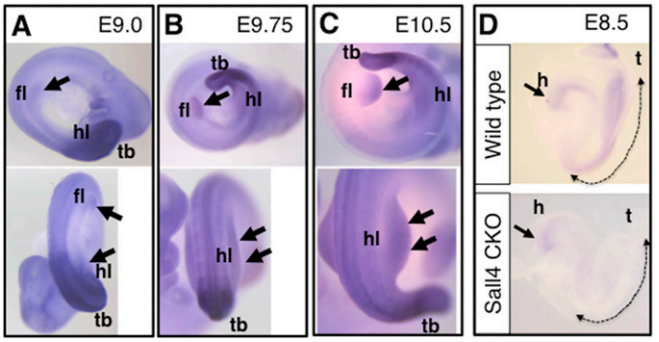

Fig. S1. *Sall4* expression pattern in wild type embryos and confirmation of early inactivation of *Sall4* by *Tcre*. (*A*–*C*) in situ hybridization of *Sall4* at E9.0 (*A*), E9.75 (*B*), and E10.5 (*C*). *Sall4* is broadly expressed at E9.0 (*A*) and E9.75 (*B*), and its expression is prominent in the tail bud region. (*C*) *Sall4* is expressed in the distal region of the forelimb bud, but is still broadly expressed in the hindlimbs. (*D*) *Sall4* in situ hybridization in wild type and *Tcre; Sall4* CKO embryos at E8.5. *Sall4* mRNA was undetectable using an exon 2 probe, which is deleted in *Sall4* cKO mice. fl: forelimb region/forelimb buds, h; head, hl: hindlimb region/hindlimb buds, tb: tail bud.

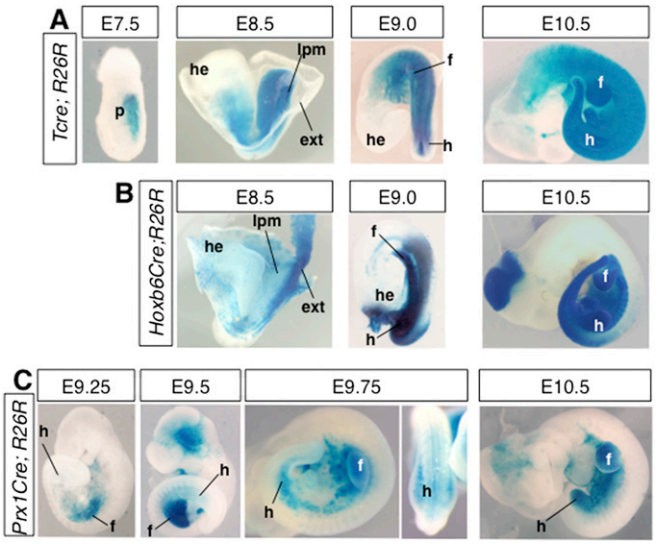

Fig. S2. Recombination by *Tcre*, *Hoxb6Cre* and *Prx1Cre*, visualized by R26R-LacZ reporter. Whole mount LacZ stained embryos of *Tcre; R26R* (*A*), *Hoxb6Cre; R26R* (*B*), and *Prx1Cre; R26R* (*C*) at indicated developmental stages. (*A*) Recombination by the *Tcre* is detected as early as E7.5 in the posterior part of the body, and broadly in E8.5 embryos. The recombined regions include forelimb-forming region/forelimb buds and hindlimb-forming region/hindlimb bud. (*B*) Recombination by the *Hoxb6Cre* was detected in the extraembryonic tissue, but not in the embryo portion at E8.5. Strong recombination was detected in the lateral plate mesoderm by E9.0. (*C*) Recombination by the *Prx1Cre* was detected in the forelimb bud at E9.25, and recombination in the hindlimb bud was detected at E9.75. Abbreviations, ext: extra embryonic tissue, f: forelimb-forming region/forelimb buds, h: hindlimb-forming region/hindlimb buds, lpm: lateral plate mesoderm, he: head, p: posterior.

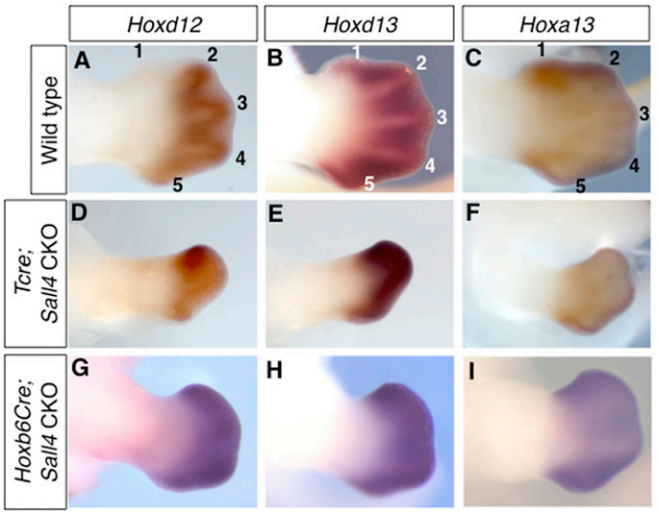

Fig. S3. Expression pattern of *Hoxd12*, *Hoxd13*, and *Hoxa13* in *Tcre; Sall4* and *Hoxb6Cre; Sall4* CKO hindlimbs. Dorsal views of E12.5 hindlimbs hybridized with indicated probes. (*A* and *B*) *Hoxd12* signals were excluded from d1 primordia, whereas *Hoxd13* signals cover all digit primordia in wild-type. (*D*, *E*, *G*, and *H*) In both *Tcre; Sall4* CKO (*D* and *E*) and *Hoxb6Cre; Sall4* CKO (*G* and *H*) hindlimbs, all digit primordia were positive for both *Hoxd12* and *Hoxd13* expression. (*C*, *F*, and *I*) *Hoxa13* expression was detected in the autopod in wild-type (C), *Tcre; Sall4* CKO (*F*), and *Hoxb6Cre; Sall4* CKO (*I*) hindlimbs. Digit primordia are numbered in wild-type images.

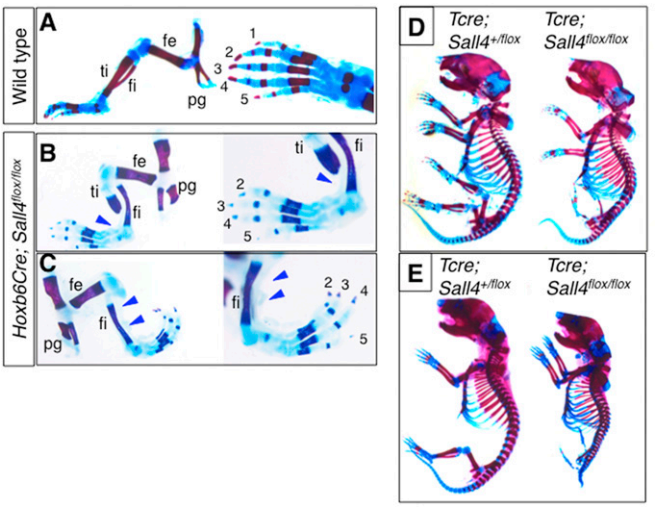

Fig. S4. Zeugopod phenotypes of *Hoxb6Cre; Sall4* CKO mutants and two examples of entire skeletal staining of *Tcre; Sall4* CKO mice. (*A*) Hindlimb skeleton of neonatal wild-type mice. (*B* and *C*) Hindlimb skeletons of a *Hoxb6Cre; Sall4* CKO neonatal mouse. Only this mutant exhibited tibia hypoplasia, denoted by arrowheads. ti: tibia, fi: fibula, fe: femur, pg: pelvic girdle. Digits are numbered as 1–5. (*D*) A typical neonatal *Tcre; Sall4* CKO mutant and a littermate. This mutant possesses three digits in hindlimbs. (*E*) A severely affected neonatal *Tcre; Sall4* CKO mutant and a littermate. The mutant exhibited reduction of the entire body size.

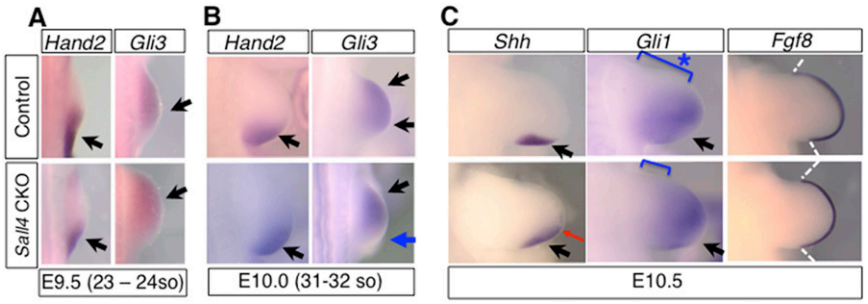

Fig. S5. Gene expression in forelimb buds of wild-type and *Sall4* CKO embryos. (*A* and *B*) *Gli3* and *Hand2* expression at E9.5 (*A*) and E10.0 (*B*). (*C*) Expression patterns of *Shh*, *Gli1*, and *Fgf8* at E10.5. *Shh* expression exhibited a subtle change, and the *Gli1*-free domain in the anterior portion exhibited a slight decrease. The expression pattern of *Fgf8* also exhibited subtle alterations.

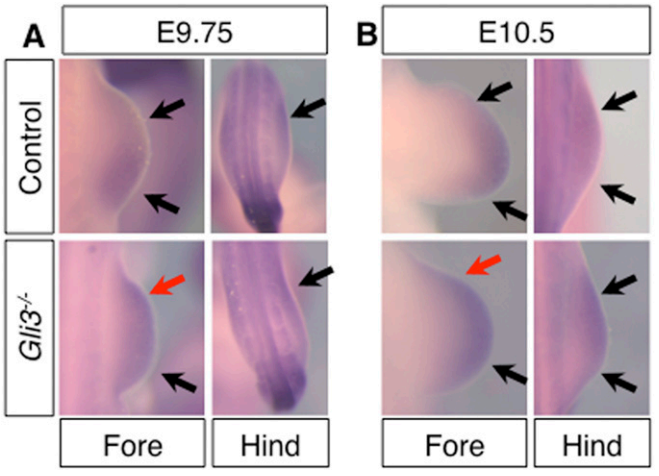

Fig. S6. Expression pattern of *Sall4* in *Gli3* mutants. In situ hybridization of *Sall4* in wild-type and $Gli3^{-/-}$ embryos at E9.75 (*A*) and E10.5 (*B*). *Sall4* expression appears to be slightly higher in the anterior part of forelimb buds (red arrows), compared with wild type. Black arrows point to normal expression.

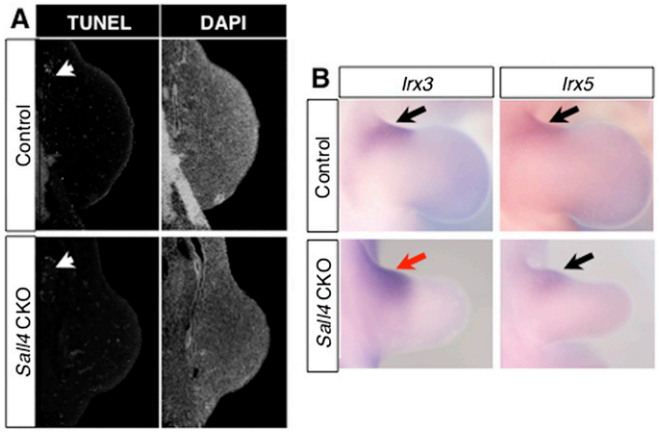

Fig. S7. Additional analyses of *Irx3/5* in *Tcre; Sall4* CKO embryos. (*A*) Comparable cell death between control and *Sall4* CKO hindlimb buds at E10.5. TUNEL and DAPI signals are shown in coronal sections. A cluster of a few TUNEL positive cells was similarly detected in the anterior-proximal region of both control and *Sall4* CKO hindlimb buds. (*B*) Expression pattern of *Irx3* and *Irx5* at E11.5 in control and *Sall4* CKO hindlimb buds. Black arrows point to normal expression, and a red arrow points to *Irx3* expression, which appears to be slightly stronger than that in wild-type control hindlimb buds.

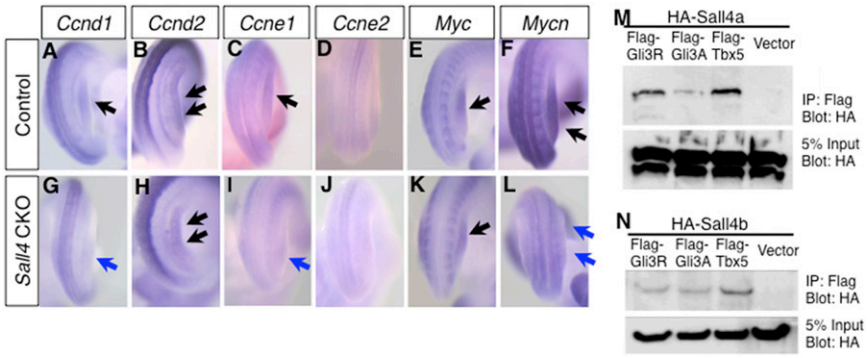

Fig. S8. Expression pattern of cell cycle progression-related genes and coimmunoprecipitation of SALL4a and SALL4b with GLI3. (*A–L*) Expression of *Ccnd1* (*A* and *G*), *Ccnd2* (*B* and *H*), *Ccne1* (*C* and *I*), *Ccne2* (*D* and *J*), *Myc* (*E* and *K*) and *Mycn* (*F* and *L*) in wild type (*A–F*) and *Sall4* CKO (*G–L*) embryos at E9.75. Black arrows and blue arrows point to normal and reduced expression, respectively. (*M* and *N*) SALL4a and SALL4b can interact with GLI3. *HA-Sall4a* (*M*) or *HA-Sall4b* (*N*) is cotransfected with Flag-tagged truncated *Gli3* (*Gli3R*), Flag-tagged full-length *Gli3* (*Gli3A*), Flag-tagged *Tbx5* or empty vector in HEK293T cells. TBX5 is used as a positive control for SALL4 interaction.

Table S1. Summary of digit number of *Sall4* mutants using different *Cre* lines

Number of digits	*Tcre; Sall4* CKO	*Hoxb6Cre; Sall4* CKO	*Prx1Cre;Sall4* CKO
1	1 (2.6%)	0 (0%)	0 (0%)
2	11 (28.9%)	0 (0%)	0 (0%)
3	23 (60.5%)	4 (7.7%)	0 (0%)
4	3 (7.9%)	26 (50.0%)	0 (0%)
5	0 (0%)	22 (42.3%)	62 (100%)
Number of limbs	38	52	62

Table S2. Summary of tibia and femur phenotype

Phenotype	*Tcre; Sall4* CKO	*Hoxb6Cre; Sall4* CKO	*Prx1Cre;Sall4* CKO
Absence of tibia	38 (100%)	2* (3.8%)	0 (0%)
Small cartilage in the stylopod	38 (100%)	0 (0%)	0 (0%)
Number of limbs	38	52	62

*The tibia was partially developed (not complete absence).

Table S3. Frequency of obtaining *Tcre; Sall4* CKO pups

Breeding scheme	Number of pups	Number of CKO pups	Frequency of neonatal mutants
♂ $Tcre^{+/Tg}$; $Sall4^{+/flox}$ ♀ $Sall4^{flox/flox}$	17	3	17.7%
♂ $Tcre^{Tg/Tg}$; $Sall4^{+/flox}$ ♀ $Sall4^{flox/flox}$	236	16	6.8%